

Shedding Light on the Matter of Abell 781

D. Wittman^{*}, William Dawson, and Bryant Benson

Physics Department, University of California, Davis, CA 95616

7 March 2022

ABSTRACT

The galaxy cluster Abell 781 West has been viewed as a challenge to weak gravitational lensing mass calibration, as Cook and dell’Antonio (2012) found that the weak lensing signal-to-noise in three independent sets of observations was consistently lower than expected from mass models based on X-ray and dynamical measurements. We correct some errors in statistical inference in Cook and dell’Antonio (2012) and show that their own results agree well with the dynamical mass and exhibit *at most* $2.2\text{--}2.9\sigma$ low compared to the X-ray mass, similar to the tension between the dynamical and X-ray masses. Replacing their simple magnitude cut with weights based on source photometric redshifts eliminates the tension between lensing and X-ray masses; in this case the weak lensing mass estimate is actually higher than, but still in agreement with, the dynamical estimate. A comparison of lensing analyses with and without photometric redshifts shows that a $1\text{--}2\sigma$ chance alignment of low-redshift sources lowers the signal-to-noise observed by all previous studies which used magnitude cuts rather than photometric redshifts. The fluctuation is unexceptional, but appeared to be highly significant in Cook and dell’Antonio (2012) due to the errors in statistical interpretation.

Key words: gravitational lensing; weak-methods; statistical-galaxies; clusters: individual: Abell 781

1 INTRODUCTION

Abell 781 is the collective name for four clusters of galaxies, not all of which are physically related. Cook and dell’Antonio (2012, hereafter C12) argue that weak lensing mass estimates of one of these clusters are substantially lower than expected based on X-ray and dynamical estimates, and that the persistence of this effect across multiple data sets from multiple telescopes presents a challenge to weak lensing calibration. In this paper we show that this claim does not stand up to closer scrutiny, and we attempt to examine the issues in a way which sheds light on weak lensing analyses in general. In this introduction we summarize previous studies to help the reader understand more specifically what the claim is, and then outline our response.

Figure 1 is a map of the region as seen by XMM. In this figure, adapted from Sehgal *et al.* (2008, hereafter S08), we have labeled the four components (East, Middle, Main, and West) as named by those authors and as labeled by C12 (C, B, A, and D respectively). The Main cluster ($z = 0.3004$, Geller *et al.* 2010) is the brightest in both galaxies and X-rays and is close to the original Abell, Corwin & Olowin (1989) position, and is therefore most strongly identified with the Abell 781 label. This cluster appears to be in a

merging state based on the offset Subcluster gas distribution labeled in Figure 1. The Middle cluster (so called because it is the middle of the three seen in archival *Chandra* data also studied by S08) is about $6'$ to the east of the Main cluster and is at the same redshift, within a few thousand kilometers per second ($z = 0.2915$, Geller *et al.* 2010). The East cluster is an additional $\sim 3'$ further east, but is at $z = 0.4265$ (Geller *et al.* 2010) and thus physically unrelated to Main and Middle. The West cluster, projected $\sim 11'$ west of Main, is at $z = 0.4273$ (Geller *et al.* 2010) and thus is physically near East, with a transverse separation of $\sim 21'$ or 7 Mpc.

Abell 781 was identified by Wittman *et al.* (2006) as a shear-selected cluster in the Deep Lens Survey (DLS; Wittman *et al.* 2002), and Abate *et al.* (2009) performed weak lensing analyses of extended X-ray sources identified in *Chandra* followup of those shear-selected clusters. They fit Navarro-Frenk-White (NFW; Navarro, Frenk & White 1997) profiles to Main, Middle, East, and Subcluster, which they called a, b, c, and d respectively. They did not fit the West cluster because, being outside the *Chandra* field of view, it did not meet their selection criteria. Because “d” in Abate *et al.* (2009) and “D” in C12 refer to different structures, we will use the S08 nomenclature to avoid confusion.

C12 were motivated to investigate West in more detail because in DLS convergence maps (Wittman *et al.* 2006, Kubo *et al.* 2009, Khiabani & DellAntonio 2008) West

^{*} E-mail: dwittman@physics.ucdavis.edu

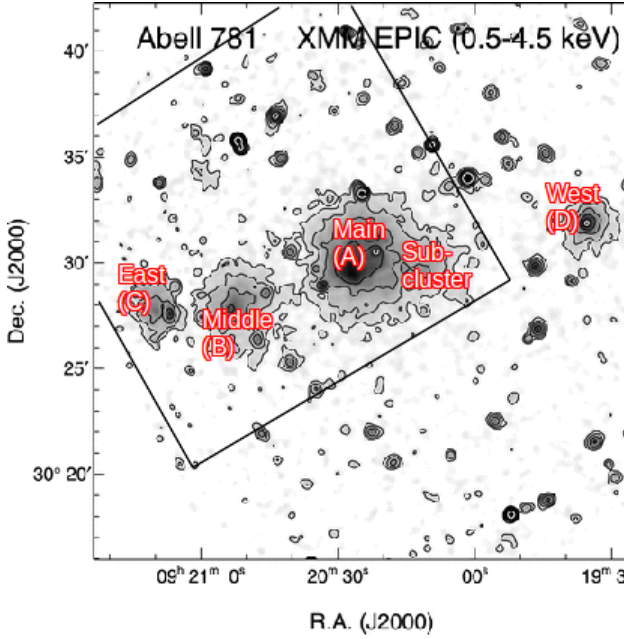


Figure 1. XMM image of the Abell 781 region, with Sehgal *et al.* (2008) labels (words) and Cook & dell’Antonio (2012) labels (letters). The smaller square indicates the *Chandra* field of view. Adapted from Sehgal *et al.* (2008).

appears at lower significance than East despite their consistent (within 1σ) X-ray temperatures and X-ray inferred masses (S08; see Table 1 and Figure 2 for a summary of all relevant mass estimates). However, C12 do not mention that S08 also fit NFW profiles to the DLS lensing data and found $M_{200} = 2.7^{+1.3}_{-1.2} \times 10^{14} M_{\odot}$ and $1.6^{+1.2}_{-1.0} \times 10^{14} M_{\odot}$ for East and West respectively¹; *i.e.*, the difference is within 1σ . Therefore, if the less prominent appearance of West on the previously published convergence maps is significant, the problem may lie in the construction or interpretation of these convergence maps rather than weak lensing generally.

As further motivation for investigating the (perceived) low weak lensing signal from West, C12 cite dynamical measurements which buttress the case for roughly consistent masses in East and West: Geller *et al.* 2010 find $\sigma_v = 754 \pm 92$ and $596 \pm 107 \text{ km s}^{-1}$ for East and West respectively. C12 converted these velocity dispersions to $M_{200} = 2.2 \pm 0.9$ and $1.1 \pm 0.7 \times 10^{14} M_{\odot}$ for East and West respectively, and converted S08’s X-ray-derived M_{500} values to $M_{200} = 2.7 \pm 0.8$ and $3.2 \pm 0.7 \times 10^{14} M_{\odot}$ for East and West respectively. With all masses in terms of M_{200} it is clear that the East dynamical mass is in excellent agreement with its X-ray mass, whereas the West dynamical mass is 2.2σ low compared to its X-ray mass. We point this out because we will show that C12’s own lensing results, properly interpreted (§2), are also about 2.2σ low compared to the X-ray model. Whether one chooses to characterize a 2.2σ deviation as rough agreement or as mild tension, the same term should apply to both the dynamical-X-ray comparison and the lensing-X-ray comparison. Also, C12 failed to note that the S08 lensing mass esti-

¹ These numbers have been converted from the M_{500} estimates of S08 to facilitate comparison with the M_{200} estimates given by C12.

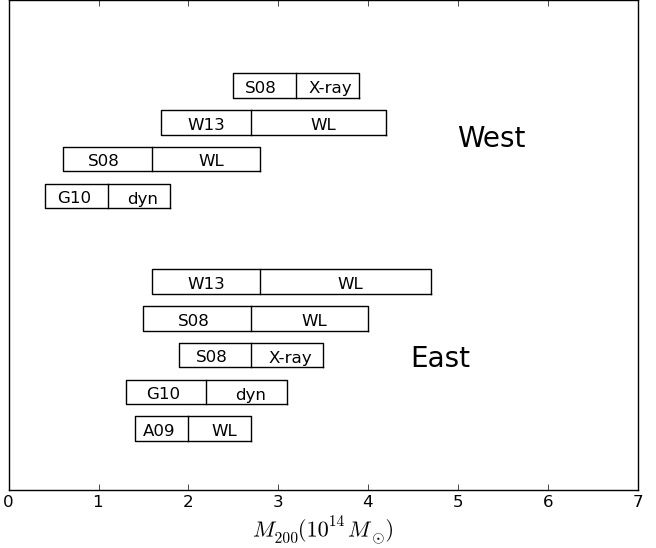


Figure 2. A graphical summary of the mass estimates for East and West (also listed in Table 1) clearly shows that all published weak lensing mass estimates are consistent with both X-ray and dynamical values. The dynamical mass estimate of West is actually the one in greatest tension with the X-ray mass estimate. The vertical line segments in each bar indicate the best-fit value and the $\pm 1\sigma$ uncertainties. Paper abbreviations are: S08, Sehgal *et al.* (2008); A09, Abate *et al.* (2009); G10, Geller *et al.* 2010; and W13, this work. Some of the estimates have been converted to M_{200} as noted in Table 1.

mate for West is actually *higher* than their dynamical mass, further weakening the argument that weak lensing mass estimates of West are persistently low.

The C12 investigation used three different weak lensing data sets from three different telescopes and cameras: the original DLS imaging, new imaging from the OPTIC camera at the WIYN telescope, and archival SuprimeCam imaging at the Subaru telescope. The OPTIC and SuprimeCam data do not cover East so C12 focused on modeling West. Rather than estimate the mass directly, they made convergence maps and then signal-to-noise (S/N) maps using bootstrap resampling of each data set. Finding relatively low S/N (1.7, 0.63, and 0.69 for DLS, OPTIC, and SuprimeCam data respectively) at the position of the West cluster, they asked whether this low weak lensing S/N is consistent with the X-ray and dynamical estimates of its mass. To answer this question, they created mock weak-lensing data sets with the mass of the West cluster constrained by the X-ray analysis. For an NFW halo with concentration parameter $c = 5$, they found that only 1.4% of DLS-like mocks yielded S/N as low as observed in their analysis of the DLS data; only 0.2% of OPTIC-like mocks yielded S/N as low as observed in their analysis of the OPTIC data; and only 1.4% of SuprimeCam-like mocks yielded S/N as low as observed in their analysis of the SuprimeCam data. They also performed a similar exercise but with the mass of the West cluster constrained by the dynamical analysis of Geller *et al.* (2010), and found somewhat better agreement, with ~ 10 –25% of mock realizations agreeing with any given data set.

Table 1. Abell 781 Mass Estimates (M_{200} in units of $10^{14} M_{\odot}$). The S08 values have been converted from M_{500} , and the Geller et al. (2010) values have been converted from velocity dispersion by C12.

Cluster	S08 X-ray	S08 Weak lensing	Abate et al. (2009) Weak lensing	Geller et al. (2010) Galaxy velocities	This Work Weak lensing
East	2.7 ± 0.8	$2.7^{+1.3}_{-1.2}$	$2.0^{+0.7}_{-0.6}$	2.2 ± 0.9	$2.8^{+1.9}_{-1.2}$
West	3.2 ± 0.7	$1.6^{+1.2}_{-1.0}$	(no data)	1.1 ± 0.7	$2.7^{+1.5}_{-1.0}$
Main	8.0 ± 1.1	$4.0^{+1.5}_{-1.3}$	$3.5^{+0.4}_{-0.6}$	4.5 ± 3.5	$6.7^{+1.4}_{-1.3}$
Middle	2.4 ± 0.6	$3.0^{+1.5}_{-1.0}$	$3.0^{+0.6}_{-0.4}$	3.5 ± 3.0	$4.3^{+1.6}_{-1.2}$

C12 concluded that the weak-lensing signal from the West cluster is anomalously low, that faulty point-spread function (PSF) correction cannot be to blame because the anomaly is observed in three independent lensing data sets, and that this anomaly provides a “challenging obstacle” for calibration of weak-lensing masses.

C12 also studied a strongly lensed arc at a radius of $\sim 7''$ around the West cluster. Although the source redshift remains unknown, C12 considered a range of likely source redshifts and concluded that the mass contained within this radius is likely to be in the range $1\text{--}1.5 \times 10^{14} M_{\odot}$. We do not use strong lensing information in this paper because our primary concern is the consistency of X-ray, dynamical, and weak lensing measurements, and because strong lensing cannot rule out any model without a secure source redshift.

In summary, a variety of physical probes by multiple investigators (X-ray and weak lensing by S08, and dynamical by Geller *et al.* 2010) support an M_{200} in the range of $1\text{--}3 \times 10^{14} M_{\odot}$. C12 do not actually infer a weak-lensing mass for the West cluster or challenge the previously published mass estimates, but find that their S/N for West is anomalously low given the models inferred from X-ray and dynamical data. Their S/N study of West was motivated by West appearing less prominently than East in previously published convergence maps, but they do not study East in their paper. Therefore, we will consider two related but distinct questions: why C12 might measure a lower S/N for West than predicted by X-ray and dynamical models, and why West might appear less prominently than East in previous convergence maps.

In §2 we answer the first question by correcting some statistical inference errors by C12 and showing that their own modeling is entirely consistent with the dynamical model and only modestly in tension with the X-ray model. In §3 present a new convergence map with the DLS data weighted using source redshift information. The roughly equal appearance of West and East in this map suggests an answer to the second question: previous convergence maps suffered from a modest ($1\text{--}2\sigma$) fluctuation in shape noise involving low-redshift sources, which is therefore suppressed when properly dewatering low-redshift sources. In §4 we summarize and discuss the implications. In Appendix A we investigate several factors which complicate the interpretation of convergence maps, particularly S/N maps. These factors do not appear to be responsible for a substantial part of the C12 result, but may be of interest to students of weak lensing.

2 STATISTICAL SIGNIFICANCE OF THE C12 RESULT

In this section we correct some errors C12 made in statistical inference and show that, according to their own modeling, the significance of their result is much lower than they imply. Throughout, we will refer to numbers from their Table 5.

First, C12 incorrectly multiplied the p-values from the different lensing data sets to obtain an overall p-value. A correct way to combine independent p-values is with Fisher’s (1925) combined probability test. Given n independent p-values p_i where $i = 1, 2, \dots, n$, a χ^2 distribution with $2n$ degrees of freedom is obtained by summing the natural logarithms of the p-values and multiplying by 2:

$$\chi^2 = -2 \sum_{i=1}^n \ln p_i$$

This χ^2 value may then be converted to a probability using standard χ^2 calculators.² Performing this test on the dynamical p-values given in C12 Table 5, we find a combined p-value of 7.4% rather than 0.3%; in Gaussian terms, a 1.4σ discrepancy. For the X-ray model in the same table, we find 0.0049% rather than $3.92 \times 10^{-5}\%$. In other words, correcting this error alone releases the tension between the lensing data and the dynamical model but not the X-ray model.

Second, the lensing data sets are not actually independent. C12 focus on the independence of the PSF corrections, but the principal source of uncertainty—shape noise, or the random pre-lensing orientations of source galaxies—is not independent across the three data sets. C12 did recognize that “the three analyses share many of the same galaxies” but this point deserves much more consideration. Shape noise is the dominant source of random error in weak lensing. The three weak lensing analyses in C12 use highly overlapping sets of sources due to similar magnitude and size cuts. Therefore, if a shape noise fluctuation appears in one lensing data set, it must appear with similar strength in the others. (An exception would be images taken at very different wavelengths, such as visible and radio, such that the pre-lensing shapes of galaxies are not highly correlated.) In other words, this dominant source of noise is highly correlated across the three data sets. The bootstrap resampling in C12 also drew

² If multiplication of p-values seems intuitively correct, consider that we expect p-values of order 0.5 for correct models. Multiplying p-values then yields a number of order 0.5^n after n independent tests. This must approach zero for large n even if the model is correct. Therefore multiplication cannot yield the correct overall p-value.

from the allowed range of X-ray (or dynamical) models, and this source of variation is also correlated across the three data sets. As a hypothetical example, if *each* lensing data set requires a model from the lowest 2% of models allowed by the X-ray fit, we should infer that the lensing data *collectively* require a model from the lowest 2% of X-ray models rather than the lowest 0.07% (the result of Fisher’s method assuming independent p-values), and certainly not the lowest 0.0008% (the result of multiplying the p-values).

Because the dominant sources of variation are highly correlated, the most reasonable overall lensing p-value to quote is that of the largest and most inclusive data set, the DLS. For the X-ray model, this value is 0.014. In Gaussian terms, this is a 2.2σ result rather than a 4.9σ result as one might infer from the “joint constraint” column of C12’s Table 5. This rises to 2.9σ if we are concerned with the OPTIC results specifically rather than the lensing results collectively. To be as fair as possible, we will quote the range of lensing results as being $2.2\text{--}2.9\sigma$ discrepant with the X-ray model. For the dynamical model, the p-value from the largest and most inclusive lensing dataset is 0.25 and in Gaussian terms the discrepancies range from $0.7\text{--}1.4\sigma$, which by most standards is good agreement.

Third, even $2.2\text{--}2.9\sigma$ is likely to be an overestimate of the X-ray discrepancy because of the halo concentration value c used by C12. A widely used approach in cluster modeling is to adopt the concentration-mass relation found in N-body simulations such as in Duffy *et al.* (2008), whose Figure 2 shows that $c \approx 4$ is the most reasonable estimate for a halo with the mass and redshift of West. C12 instead chose two illustrative values: $c = 10$ for their Table 4 and $c = 5$ for their Table 5. However, $c = 10$ is highly disfavored according to the Duffy *et al.* (2008) results. This is why we have focused on C12’s results for $c = 5$ (their Table 5). Furthermore, because the tension between the X-ray model and the lensing data is substantially reduced as the model changes from $c = 10$ to $c = 5$, the tension is likely to be reduced even more for a halo with $c = 4$. At the least, C12 should have considered a range of concentrations extending below 5, and this would have reduced the tension between the X-ray and lensing results.

In summary, the correct interpretation of the lensing analyses in C12 is that they are *at most* $2.2\text{--}2.9\sigma$ low compared to the X-ray model, and in good agreement with the dynamical model. These results are consistent with the rest of the literature. C12 cite Abate *et al.* (2009) as finding a best-fit NFW mass of $M_{200} = 0.0^{+0.5}_{-0.0} \times 10^{14}$ as supporting evidence for the low signal in “A781D.” As noted in §1, however, Abate *et al.* (2009) did *not* fit the West cluster; rather, their “d” refers to S08’s Subcluster which is an extension of the gas in the Main cluster. Once this mistake is rectified it is clear that the only published weak lensing mass estimate of West is the one by S08, which C12 overlooked and which is actually *higher* than the dynamical estimate.

We have demonstrated the consistency of weak lensing results with the X-ray and dynamical results simply by considering the nonindependence of data sets and by a careful reading of the literature. Yet a new question arises: why have different analyses of the same DLS lensing data resulted in

even $\sim 1\sigma$ variations in our view of West?³ Given that these analyses use the same data set, one would expect much less variation unless the choice of analysis procedure is the dominant source of variation; and in that case, we should identify which choices in the analysis procedure are so important. We investigate this issue in the next section.

3 CONVERGENCE MAP WITH SOURCE REDSHIFT WEIGHTING

The DLS has photometric redshifts (Schmidt & Thorman 2013) which were not available or not used for the convergence maps made by Wittman *et al.* (2006), Khiabani & DellAntonio (2008), and Kubo *et al.* (2009). Since we know the cluster redshift, we can use the source photometric redshifts to optimize sensitivity to lenses at this redshift. Photometric redshifts not only provide a much more highly tailored cut against foreground objects compared to the magnitude and size cuts used by C12, but they can also be used to lower the weight of sources which are just behind the cluster and which are therefore lensed inefficiently. (Those sources are lensed more efficiently by structures at lower redshift than the target cluster.) This is related to weak lensing tomography: in tomography we make maps from a series of source redshift bins to explore changes in structure as a function of redshift, whereas here we weight the source redshifts to highlight structure at a known redshift.

Following Dawson *et al.* (2012), we note that the shear γ is proportional to a ratio of angular diameter distances:

$$\gamma \propto \frac{D_{ls}(z_l, z_s) D_l(z_l)}{D_s(z_s)} \mathcal{H} \left(\frac{z_s}{z_l} - 1 \right)$$

where D_l , D_s , & D_{ls} are the angular diameter distances from observer to lens, observer to source, and lens to source, respectively, z_l and z_s are the lens and source redshifts respectively, and \mathcal{H} is the Heaviside step function. A matched filter for lenses at $z_l = 0.43$ would then weight each source by the distance ratio on the right-hand side with z_l set to 0.43. However, for each source z_s is a probability distribution $p(z)$ rather than a single number. We integrate over this distribution to obtain the redshift-dependent part of the weight for each galaxy:

$$w = \int \frac{D_{ls}(z_l, z_s) D_l(z_l)}{D_s(z_s)} \mathcal{H} \left(\frac{z_s}{z_l} - 1 \right) p(z_s) dz_s$$

where z_l is fixed at 0.43. We also weight by the inverse variance of the galaxy’s shear measurement.

The resulting convergence map of the Abell 781 region for $z_l = 0.43$ is shown in Figure 3, top. In contrast to the maps of Wittman *et al.* (2006), Khiabani & DellAntonio (2008), and Kubo *et al.* (2009), the West cluster is about as prominent as the East cluster, with $S/N = 3.0$. We attribute this to the source redshift weighting. Assigning different weights to each source effectively resamples the data and results in a different realization of shape noise. Thus,

³ For example, the C12 S/N is on the low side of estimates from the dynamical model whereas the S08 lensing model is on the high side of the dynamical model, and C12 were themselves motivated by convergence maps showing West as less prominent than the equally-massive East.

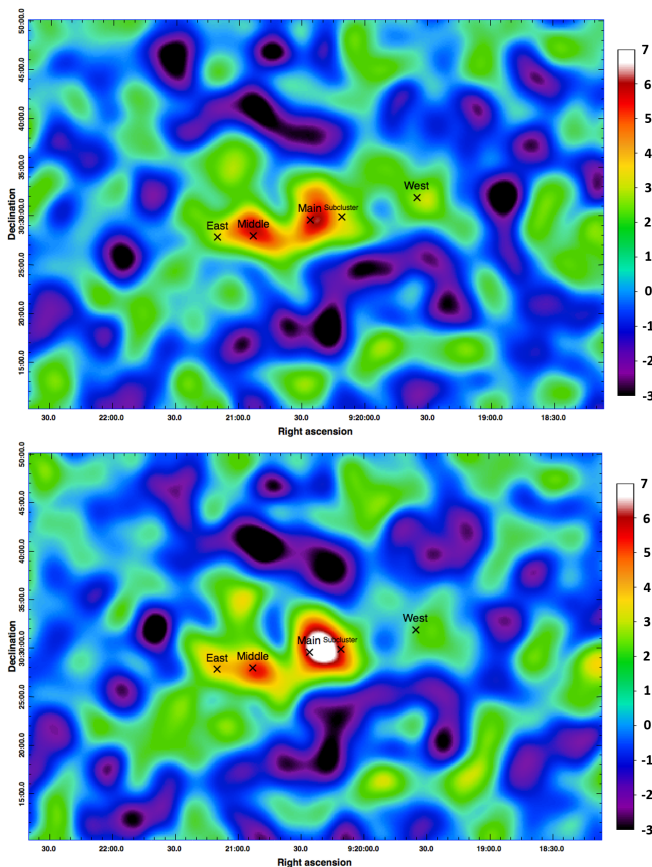


Figure 3. Top: Convergence map (in units of signal-to-noise, based on 100 bootstrap realizations) of the Abell 781 region made with photometric redshift probability density ($p(z)$) weighting. The West cluster is clearly visible at about the same signal-to-noise as the East cluster. Bottom: the same map made with the C12 magnitude cuts rather than the $p(z)$ weighting. Here, as in the convergence maps which motivated the C12 investigation, West appears at lower signal-to-noise than East. The difference is consistent with shape-noise fluctuations (ie, chance alignments of source galaxies) at the low redshifts which are downweighted by the redshift weighting.

this simple analysis choice can influence the results about as much as the dominant source of noise because it resamples the dominant source of noise. To confirm this, we remade the map with the C12 magnitude cuts rather than source redshift weighting and indeed the S/N of West declines to 2.4 while that of East increases slightly (Figure 3, bottom).

Therefore, a plausible scenario which accounts for all the published results is that the assumption that all sources share the same effective distance ratio happens to bias the West signal low. This scenario does not require any specific source redshift distribution near the West line of sight; it merely requires that the random orientations of lower-redshift sources (including those behind the West cluster but at low distance ratio) happen to reduce the measured tangential shear. Because the signal-to-noise of East and West on these maps are already rather low, a mere $1-2\sigma$ shape-noise fluctuation along the West line of sight would be sufficient to nearly remove West as a peak on the map. This scenario would also explain the fact that S08, who used photometric redshift weighting in their weak lensing analy-

sis, did not find an anomalously low weak lensing mass for West.

Another potentially important difference between S08 and C12 is that S08 employed a model-fitting approach, whereas C12 (and the map makers cited by C12) employed a data-smoothing approach. For completeness, we also present the results of a model-fitting approach. We fit four simultaneous NFW models to the DLS weak lensing data with full $p(z)$ weighting and with centers fixed by the X-ray locations (other details of the fitting procedure are as described in Dawson *et al.* 2012). For all subclusters, the resulting masses (Table 1) agree (within 1σ) with all previous mass estimates. Our mass estimates are on average slightly higher than the weak lensing estimates of S08, which we attribute to our use of the full $p(z)$ rather than the one-point redshift estimates used by S08; Wittman (2009) showed that the one-point estimates are biased tracers of the underlying $p(z)$. In Appendix A we show that the data-smoothing approach is subject to some types of errors to which the model-fitting approach is immune. However, the two smoothed maps we present here demonstrate that the choice of a data smoothing approach by itself does not result in the reduced prominence of West. The choice of redshift weighting is more important.

Although the previously published maps served as motivation for the C12 investigation of the S/N of West in multiple lensing data sets, C12 do not themselves compare East and West because East is outside the footprint of their new data. Therefore, we have fully addressed the two independent but related issues with a single hypothesis which fits all the existing results. A $1-2\sigma$ low-redshift shape noise fluctuation could (1) nearly remove West as a peak in previously published convergence maps, but allow it to appear as a 3σ peak when sources are properly weighted by distance ratio (as seen in this work and in S08); and (2) explain why the weak lensing S/N modeling of C12 is $\sim 1\sigma$ low compared to the dynamical model while S08 found a weak lensing mass slightly higher than the dynamical model.

4 SUMMARY

C12 focus on ruling out PSF modeling errors as an explanation for the weak lensing S/N they measure for the West cluster, and they succeed in ruling this out by considering three independent data sets. However, their conclusion that “A strong discrepancy remains between the [weak] lensing mass of A781D and the mass estimates from spectroscopic and X-ray measurements” is not at all justified after correcting the following errors in interpreting the statistics and the literature:

- their three lensing constraints are very far from independent so that the joint constraint found by C12, indicating a $\sim 5\sigma$ deviation from the X-ray model, should actually be considered at most a $2.2-2.9\sigma$ result. The actual significance must be less than this because C12 overestimate the halo concentration parameter and do not account for the uncertainty in the halo concentration.
- recognizing the nonindependence of the lensing constraints also removes any tension with the dynamical model. The tension with the dynamical model is also removed *even if* the lensing data sets are independent and one simply uses the correct method for combining independent p-values.

- C12 misread the Abate *et al.* (2009) weak lensing estimate of the Subcluster as applying to the West cluster. In fact, the only previously published weak lensing mass estimate of the West cluster (S08) is actually *higher* than the dynamical estimate.

The S08 weak lensing mass estimate is on the high side of the dynamical estimate whereas the modeling of C12 shows it to be on the low side. Although this difference is not statistically significant, one would not expect even a 1σ difference between two studies using the same underlying (DLS) data set unless some systematic analysis choice had a substantial influence. We identify this analysis choice as the use of distance ratio weighting using source photometric redshifts. A $1-2\sigma$ shape-noise fluctuation at low redshift would affect the C12 result and the previously published convergence maps which motivated C12 (Wittman *et al.* 2006, Khiabani & Dell’Antonio 2008, and Kubo *et al.* 2009), but would be nearly invisible to the method of S08 and the weighted convergence map we present here.

ACKNOWLEDGMENTS

We thank Ian Dell’Antonio for kindly providing data analysis files and useful comments. Funding for the Deep Lens Survey has been provided by Lucent Technologies Bell Labs, UC Davis, and NSF grants AST 0441072 and AST 0134753. Observations were obtained at Cerro Tololo Inter-American Observatory and Kitt Peak National Observatory. CTIO and KPNO are divisions of the National Optical Astronomy Observatory (NOAO), which is operated by the Association of Universities for Research in Astronomy, Inc., under cooperative agreement with the National Science Foundation.

APPENDIX A: INTERPRETING WEAK LENSING S/N MAPS

This Appendix addresses some issues which are potentially important in the type of modeling conducted by C12 but which turned out to be subdominant in resolving the mystery of Abell 781 West. Most discussions of weak lensing errors, including that of C12, focus on PSF modeling and shape measurement, but there is much more to consider:

- unmodeled foreground source contamination: C12 use COSMOS (Scoville *et al.* 2007) data to model their source redshift distribution, without explicitly accounting for the presence of a rich cluster (Main) in the foreground of West.
- effect of nearby structures: East may appear more prominent than West on a smoothed convergence map because shear from Middle is smoothed into East (to a far greater extent than shear from Main is smoothed into West).
- spatially varying noise: the bright star projected near West causes a loss of source galaxies and therefore an increase in noise in the region around West. In the data-smoothing approach, missing data in high-signal regions also causes a loss of signal. The simulation approach adopted by C12 is capable of including these effects, but there is no evidence that C12 included them.
- map pixelization: C12 used large ($1.5'$) pixels and West’s X-ray peak is near a pixel corner, so we examine the effect of a $\sim 1'$ miscentering.

Although many of these differences turned out to have little effect on this particular result, we describe them briefly here in the hope that students of weak lensing will benefit from the discussion. In several places, we point out advantages of a model-fitting approach over a data-smoothing approach.

A1 Unmodeled foreground source contamination

C12 imposed more or less standard size and magnitude cuts on their sources. Recognizing that these cuts would not eliminate all foreground and cluster member galaxies, they modeled the contamination by imposing the same cuts on the COSMOS catalog, ray-tracing the resulting source catalog through a model lens, and comparing the simulated S/N maps to their measured S/N maps. But the presence of Main in West’s foreground implies the presence of more foreground galaxies than in a random field. If these galaxies were present in the final source catalog they would dilute the lensing signal. To test for this, we examined the photometric redshift distribution of sources surviving their cuts in random DLS regions versus in the area around West. We did not find that the area around West contained an excess of sources at the redshift of Main, after the C12 cuts. This implies that the maximum source size imposed by C12 was effective in eliminating Main galaxies. Therefore Main’s contribution to foreground contamination, although potentially an important unmodeled effect, appears to have played little role in practice.

A2 Effect of nearby structures

The data-smoothing approach does not allow us to distinguish between shear from different sources. Middle is projected only $3'$ from East so shear from Middle is smoothed into East’s area. Shear from Main must also be smoothed into West’s area, but given the larger separation ($11'$) this should be a much smaller effect. For some choice of smoothing scales, this could explain why East appears more prominent on convergence maps but would not explain why the shear observed in the direction of West falls short of model predictions.

We tested this hypothesis by generating mock source catalogs with shear representing different cluster geometries (single cluster, two clusters with the East-Middle separation, or two clusters with the Main-West separation), and creating convergence maps with the same *flatmap* code and smoothing scales used by C12. We did not find a substantial boost for the mock East cluster above that of West; in fact the boost in either case was minimal. Therefore this effect does not answer the question raised by C12, but readers should be aware of the possibility when interpreting smoothed maps. When considering multiple lenses projected near each other, a simultaneous model-fitting approach (S08, Abate *et al.* 2009) facilitates a better distinction between the contributions of different lenses.

In general, weak lensing analyses should remain cognizant of the uncertainty due to less easily identifiable foreground and background structures, which can be tens of percent (Rasia *et al.* 2012 and references therein). C12 did recognize this and were able to discount it using the redshift survey of Geller *et al.* (2010) in this field.

A3 Spatially varying noise

Because C12's primary claim is that the S/N of West is low, it is important to examine not only effects on signal but also sources of noise. Bright stars increase noise locally by masking background galaxies, and the West cluster has a bright ($V = 11.9$) star only $\sim 54''$ away. The size of the effect depends on the details of the size of the masked area, its geometry relative to the lens center and other structures in the region, and (for the data-smoothing approach) the filter used to smooth the data. A loss of data will increase uncertainty for both model-fitting and data-smoothing approaches, but the data-smoothing approach is uniquely sensitive to a loss of signal: if the unobserved area falls near the lens center, the smoothed shear field will be biased low. In contrast, unobserved area is simply ignored when fitting a model, so that no bias can be introduced. (However, note that VanderPlas *et al.* 2012 have proposed a method for interpolating shear over masked areas.) The sizes of these effects depend on the geometry, and simulations are the best tool for assessing the impact.

We simulated the effect of the lost area for the given geometry, using a $1'$ radius mask around the star. (C12 did not explicitly use a mask, but scattered light from the star does remove some area, and we chose a large mask as a starting point.) We created mock catalogs with shear imprinted by four singular isothermal sphere lenses arranged in the geometry of the Abell 781 region and created convergence maps with the same *fiatmap* code used by C12, with and without placing a mask near the West cluster. We did not find a significant effect on the S/N of the mock West cluster for this set of parameters. A possible contributing factor is that the Main cluster and the mask are on opposite sides of the the West cluster. This means that when tangentially averaging around the West cluster, galaxies which are more sheared by the Main cluster are retained while galaxies which are less sheared by the Main cluster are masked. Thus two weaknesses of the data-smoothing approach—sensitivity to neighboring lenses and to missing data—mostly cancel each other here.

A4 Convergence map pixelization

A pixelized map represents some function of the shear field *evaluated at the center of each of its pixels*. If the peak of the lens happens to be near the corner of a pixel, this miscentering will result in a smaller pixel value than if the peak of the lens happens to be at the center of a pixel. Normally this is not a large effect because one can choose to make the pixel size as small as desired. Small pixels do not improve the angular resolution of the map beyond what is supported by the smoothing scale, but they do prevent underestimation of the S/N due to miscentering. C12 used large ($1.5'$) pixels and the X-ray position of West is near the corner of one pixel, so the miscentering hypothesis must be investigated.

We again used mock catalogs to estimate the size of this effect for the particular geometry here and for a singular isothermal sphere (SIS) model as an extreme example (less peaky profiles produce a smaller miscentering effect). C12 provided us with a variety of maps with a range of smoothing parameters. We calculated the reduction in signal due to miscentering for each choice of smoothing parameters, and

found that it ranged from 1–30%. In other words, the measured signal could be as small as 70% of the expected signal due to the miscentering effect, but only if the true shear profile is as peaky as an SIS. The miscentering effect could therefore play a small role in suppressing the S/N measured by C12. However, if C12's mock observations correctly incorporated West's X-ray peak location relative to their map grid, then this effect is already included in their S/N modeling results and therefore would not alter their results.

REFERENCES

- Abate, A., Wittman, D., Margoniner, V. E., et al. 2009, *ApJ*, 702, 603
- Abell, G. O., Corwin, H. G., Jr., & Olowin, R. P. 1989, *ApJS*, 70, 1
- Cook, R. I., & Dell'Antonio, I. P. 2012, *ApJ*, 750, 153
- Dawson, W. A., Wittman, D., Jee, M. J., et al. 2012, *ApJL*, 747, L42
- Duffy, A. R., Schaye, J., Kay, S. T., & Dalla Vecchia, C. 2008, *MNRAS*, 390, L64
- Fisher, R.A., Statistical Methods for Research Workers, Oliver and Boyd (Edinburgh, 1925)
- Geller, M. J., Kurtz, M. J., Dell'Antonio, I. P., Ramella, M., & Fabricant, D. G. 2010, *ApJ*, 709, 832
- Khiabianian, H., & Dell'Antonio, I. P. 2008, *ApJ*, 684, 794
- Kubo, J. M., Khiabianian, H., Dell'Antonio, I. P., Wittman, D., & Tyson, J. A. 2009, *ApJ*, 702, 980
- Navarro, J. F., Frenk, C. S., & White, S. D. M. 1997, *ApJ*, 490, 493
- Rasia, E., Meneghetti, M., Martino, R., et al. 2012, *New Journal of Physics*, 14, 055018
- Schmidt, S. J., & Thorman, P. 2013, *MNRAS*, 431, 2766
- Scoville, N., Abraham, R. G., Aussel, H., et al. 2007, *ApJS*, 172, 38
- Sehgal, N., Hughes, J. P., Wittman, D., et al. 2008, *ApJ*, 673, 163
- VanderPlas, J. T., Connolly, A. J., Jain, B., & Jarvis, M. 2012, *ApJ*, 744, 180
- Wittman, D. 2009, *ApJL*, 700, L174
- Wittman, D., Dell'Antonio, I. P., Hughes, J. P., et al. 2006, *ApJ*, 643, 128
- Wittman, D. M., Tyson, J. A., Dell'Antonio, I. P., et al. 2002, *Proc. SPIE*, 4836, 73